International Journal of Thermophysics, Vol. 8, No. 2, 1987

Experimental Investigation of Extinction Properties and Thermal Conductivity of Metal-Coated Dielectric Fibers in Vacuum

H. Reiss,[1] F. Schmaderer,[1] G. Wahl,[1] B. Ziegenbein,[1] and R. Caps[2]

Received May 13, 1986

This paper describes first experimental steps of an attempt to replace evacuated multifoils by metal-coated dielectric fibers as a new superisolation. Calculations of the Rosseland mean of spectral extinction coefficients for thin highly relective fibers show that radiation transport can be reduced to the same extent that is achievable with multifoils. Experimental results of extinction coefficients and thermal conductivity of Al-coated glass fibers are reported. Apparently, the metal coating does not increase seriously the small solid thermal conductivity of pure glass fibers. The procedure for optimizing this insulation is thus reduced to an optimization of its extinction properties.

KEY WORDS: anisotropic scattering; fibers; insulations; low-pressure CVD; low temperatures; Mie theory; scaled diffusion law; spectral extinction coefficient; thermal conductivity; totally reflecting fibers.

1. INTRODUCTION

Evacuated highly reflective multifoils up to now have delivered thermal insulations of lowest heat transfer rates in cryophysics and at high temperatures. However, a number of partly severe requirements with regard to material selection, preparation, mounting, and long-term performance have to be fulfilled in order to exploit fully their excellent thermal performance.

In this paper, we describe an approach to a *continuous*, evacuated fiber insulation which could not only replace evacuated foils in their radiative aspects but also avoid the enormous ratio of lateral to normal conduction,

[1] Brown, Boveri & Cie AG, Zentrales Forschungslabor, D-6900 Heidelberg, Federal Republic of Germany.

[2] Physikalisches Institut der Universität, D-8700 Würzburg, Federal Republic of Germany.

0195-928X/87/0200-0263$05.00/0

permit simpler handling and mounting, and allow residual gas pressures that are a factor of about 10 to 100 higher than required for evacuated multifoils.

It is well known that attempts to replace evacuated multifoils by evacuated metal-coated microspheres were of only limited success. The thermal radiation resistance of metal-coated spheres was hardly increased compared to that of pure dielectric spheres [1, 2].

A comparison of the solid conductivities λ_{sc} of spheres in bulk or of a regular array of fibers

$$\lambda_{sc}^{\text{sphere}} = \frac{3.44(1-\Pi)^{4/3}\,\lambda_T\, p^{1/3}}{[Y/(1-\mu^2)]^{1/3}} \tag{1a}$$

$$\lambda_{sc}^{\text{fiber}} = \left[\frac{16(1-\Pi)^2}{\pi^2}\right]\left\{\frac{\lambda_T}{(1/1.86Ap^{1/3}) + [1/4(1-\Pi)]}\right\} \tag{1b}$$

as given in Ref. 3 shows that if we assume exactly the same porosity and material parameters for both geometries, the solid thermal resistance of *fibers* should be better than the resistance of spheres because of the term $1/[4(1-\Pi)]$ in the denominator of Eq. (1b) and a numerical factor. In Eqs. (1a and b), $1-\Pi$ denotes the porosity, λ_T is the thermal conductivity of the solid material the spheres or fibers are made from, and p is the specific load on the sample. The factor A is used to calculate the contact radius between two fibers according to Hertz' formula, $A = \{(1-\mu^2)/[Y(1-\Pi)^2]\}^{1/3}$. In these expressions Y is the Young's modulus of elasticity and μ is Poisson's number. It remains to be shown that thin metal-coated fibers also yield a better extinction performance than metal-coated microspheres. This is the subject of this paper.

2. EXTINCTION COEFFICIENT OF THIN FIBERS

It is well known from recent literature [4] that extinction cross sections of very thin fibers made of materials of large complex indices of refraction can reach values that are orders of magnitude higher than those prepared from a dielectric material. However, the heat flow by solid conduction through pure metal fibers could be too large to be comparable with the performance of an uncompressed multifoil insulation. Instead of pure metal fibers, the application of metal-coated *dielectric* fibers could lead to a lower solid thermal conductivity of the fiber insulation.

The extinction properties of metal-coated dielectric fibers will be regarded in the following as those of pure, homogeneous, metal fibers, i.e., we consider the dielectric core as a small (negligible) perturbation of the homogeneous metal case. The skin depth for the electric field is, e.g., at

wavelengths Λ above 5 μm, for the metals Ag and Al, below 0.02 μm, which is easily fulfilled with the coatings applied in the experiments (see below).

The extinction coefficient E_{Fiber} of a board of loosely packed evacuated metal fibers that permits a radiative flow $\dot{q}_{\text{rad}}$ equal to or smaller than through a stack of $N = 50$ metal foils in high vacuum can be estimated as follows: if T_1 and T_2 are the boundary temperatures of a plane layer of $D = 30$-mm thickness, $\varepsilon_F = 0.05$ the emission coefficient of thermal radiation of the metal foils, whereas $\varepsilon_W = 1$ is the wall emissivity, and $n^2 = 1.1$ the squared real part of the (complex) far-infrared refractive index (effective value of the highly dispersed fibers assuming a porosity $\Pi = 0.95$), then with the Stefan–Boltzmann constant σ and the well-known expression for the $\dot{q}_{\text{rad}}$ of foils [3] and the diffusion model solution for fibers assuming isotropic scattering, we have to fulfill

$$\dot{q}_{\text{rad}}^{\text{foil}} = \frac{\sigma(T_1^4 - T_2^4)}{1 + N(\eta_W/\eta_F)} \geqslant \frac{4\sigma n^2(T_1^4 - T_2^4)}{3E_{\text{Fiber}} D} = \dot{q}_{\text{rad}}^{\text{fiber}} \tag{2}$$

i.e., $E_{\text{Fiber}} \geqslant 10^5\ \text{m}^{-1}$. The η_W and η_F in Eq. 2 denote reduced emissivities, $\eta = \varepsilon/(2 - \varepsilon)$. In the following we investigate how this goal can be reached using spectral values of the complex refractive index of a typical highly reflective metal (Al or Ag) for a calculation of the extinction cross section Q_{ext} from Mie theory and of the Rosseland mean E_R of spectral values E_Λ of the extinction coefficient taking into account anisotropic scattering. Note that this procedure does not double the investigations made in Ref. 5, where radiative flow $\dot{q}_{\text{rad}}$ was calculated. Radiative flow $\dot{q}_{\text{rad}}$ or radiative conductivity λ_{rad} are quantities that are not directly measurable, whereas extinction coefficients can easily be detected.

A computer program was written for calculating Q_{ext} (following closely recommendations and program samples made in Ref. 6) and for a scaled value E_R^* of E_Λ in dependence of temperature. Since the fibers will be arranged in multilayers with their fiber axes oriented perpendicularly to the temperature gradient, it is sufficient to consider only the case of perpendicular incidence ($\phi = 0$) of unpolarized radiation on infinite cylinders. It has been shown [7, 15] that the enormous computational effort arising from an explicitly calculated average over all tilt ϕ angles as done in Ref. 5 can be simulated successfully by multiplication of the result for perpendicular incidence by simple constants. Furthermore, for totally reflecting cylinders, the solution for the scattering coefficients for perpendicular or inclined incidence coincide (apart from a factor cos ϕ modifying the fiber radius) because the cross modes disappear [8] (polarization effects can be neglected [9]).

Spectral values of $Q_{\text{ext},\Lambda}$ are calculated using the usual expressions for

the scattering matrix elements T_1, T_2 (see, e.g., Ref. 6) evaluated at the scattering angle $\theta = 0$ (Λ denotes the wavelength). Furthermore, we calculated the scattering cross sections $Q_{\mathrm{sca},\Lambda}$ in order to determine the spectral values Ω_Λ of the albedo of single scattering. This was done for pure metal and, for comparison, for pure dielectric fibers using spectral values of the complex refractive index for Ag [10] and glass [11]. If d denotes the fiber diameter, Fig. 1 shows $Q_{\mathrm{ext},\Lambda}$ in dependence of the parameter $x = \pi$

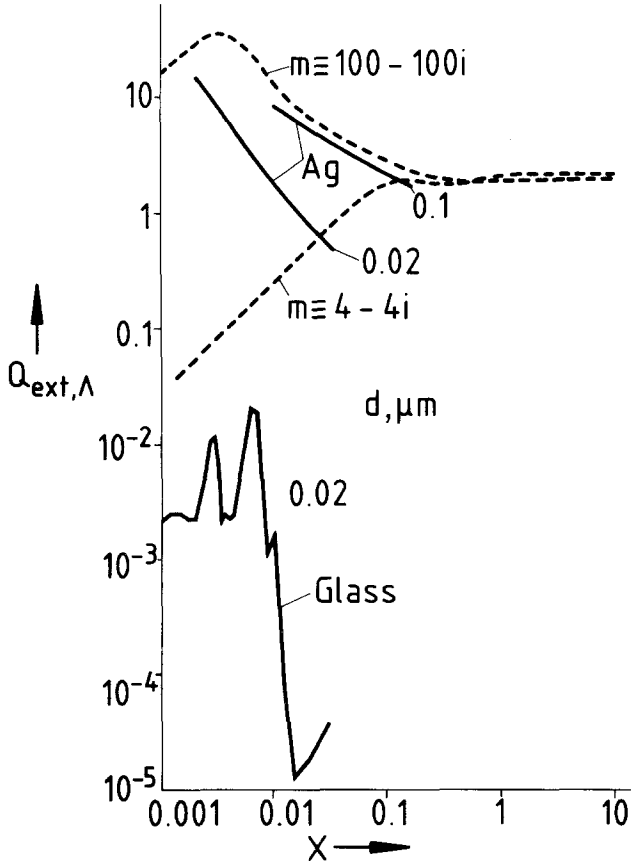

Fig. 1. Relative extinction cross sections, $Q_{\mathrm{ext},\Lambda}$, of thin fibers made of a metal (Ag) or glass (solid curves) irradiated by unpolarized radiation (perpendicular incidence), in dependence of the parameter $x = \pi d/\Lambda$ (Λ denotes the wavelength; d, the fiber diameter). Calculations are performed using spectral values of the complex index of refraction, m. For the solid curves d was kept constant. Dashed curves are given for two arbitrarily chosen values of m for comparison with the calculations made in Ref. 5 (d or Λ variable, m constant).

d/Λ. The extinction cross section, $Q_{\text{ext},\Lambda}$, and specific extinction coefficient, E_Λ/ρ, of these fibers are related by

$$E_\Lambda/\rho = \frac{4Q_{\text{ext},\Lambda}}{\rho_0 \Lambda x} = \left(\frac{4}{\pi\rho_0}\right)\left(\frac{Q_{\text{ext},\Lambda}}{d}\right) \tag{3}$$

If $\rho = 200\ \text{kg} \cdot \text{m}^{-3}$, the above-estimated goal [see Eq. (2)] amounts to an average $E/\rho \simeq 0.5\ \text{m}^2 \cdot \text{g}^{-1}$ (ρ denotes the density of the fibers; ρ_0, the density of the solid material). Compared with the goal, it follows from Fig. 1 that metal fibers with small diameters, d, obviously lead to very large E_Λ/ρ at a fixed wavelength, Λ, and small x.

It has been shown [12, 15] that the albedo Ω_Λ of metal *and* glass fibers goes to zero (i.e., pure absorption) if the fiber diameter is very small ($d \leqslant 0.1\ \mu\text{m}$). Otherwise there is a considerable amount of scattering of which the phase function must be investigated.

If we use the diffusion expression for $\dot{q}_{\text{rad}}$ [Eq. (2)] and the additive approximation (with $\dot{q}_s$ for the solid conduction part of the total heat flow, $\dot{q}$, through evacuated fibers)

$$\dot{q}_s = \dot{q}_{so} + \dot{q}_{sc}$$

$$\dot{q} = \dot{q}_s + \dot{q}_{\text{rad}}$$

($\dot{q}_{so}$ accounts for a contact heat flow which exists also in the absence of an external load, p), the total thermal conductivity, λ, reads (assuming $n^2 = 1$)

$$\lambda = \lambda_{so} + \lambda_{sc} + \lambda_{\text{rad}}$$

$$= \lambda_s + \frac{4\sigma T^{*3}}{3E^*} \tag{4a}$$

$$= \alpha + \beta T^{*3} \tag{4b}$$

Here E^* denotes an effective (scaled) value of the wavelength-averaged extinction coefficient E in the layer,

$$E^* = E(1 - \Omega\,\overline{\cos\theta}) \tag{5}$$

in the case of an arbitrary (wavelength-averaged) albedo, Ω. The factor $\overline{\cos\theta}$ accounts for anisotropic scattering and is defined as the weighted mean of the cosine of the scattering angle θ with respect to the phase function, $p(\theta)$:

$$\overline{\cos\theta}_\Lambda = \frac{\int \cos\theta_\Lambda\, p(\theta)_\Lambda\, d\omega}{\int p(\theta)_\Lambda\, d\omega} \tag{6}$$

Note that $\overline{\cos\theta} = 1, 0, -1$ corresponds to complete forward, isotropic, or backward scattering, respectively. In this definition, $d\omega$ is a solid-angle element.

It has been shown [13, 15] that the simple diffusion model yields highly accurate results for $\dot{q}_{\text{rad}}$ also in the case of a strongly anisotropic scattering medium if the effective value E^* of the extinction coefficient is used in Eq. (4a).

The quantity T^{*3} denotes a radiation temperature, $T^{*3} = (T_1^2 + T_2^2)(T_1 + T_2)$. According to Eq. (4b), the total thermal conductivity, λ, should be linear in T^{*3}, if λ_s and E^* are independent of temperature. Thus from a (λ, T^{*3}) plot, λ_s and E^* can be extracted from the intercept and slope of a linear least-squares fit to the data, if the assumption of constant λ_s and E^* is valid. The obtained λ_s and E^* have to be interpreted as mean values averaged over the total insulation thickness. We use this representation of data for the analysis of conductive and radiative components of the total λ.

References 12 and 15 illustrates that the average $\overline{\cos\theta}$ for metal and glass-fiber diameters with $d \geqslant 1$ μm increases to values between 0.1 and 1. This leads to a considerable decrease in the E_Λ/ρ values expected from Fig. 1 since Ω_Λ also approaches 1. Figs. 2 and 3 show the calculated E_Λ^*/ρ

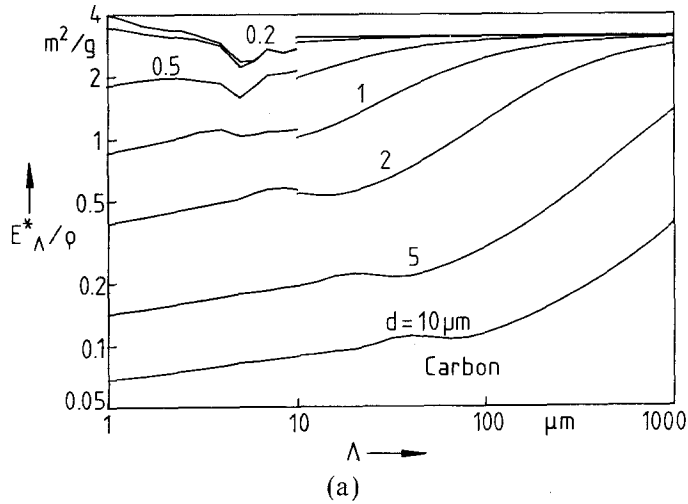

Figs. 2a, b, c. Effective values E_Λ^*/ρ of the specific extinction coefficient E_Λ/ρ of fibers made of (a) carbon, (b) Al or (c) Ag (linear scale) in dependence of wavelength, Λ, and for different fiber diameters, d. ρ denotes the density of the fibers (E_Λ^*/ρ takes into account anisotropic scattering). (Figs. 2a and 2b are from Ref. 15.)

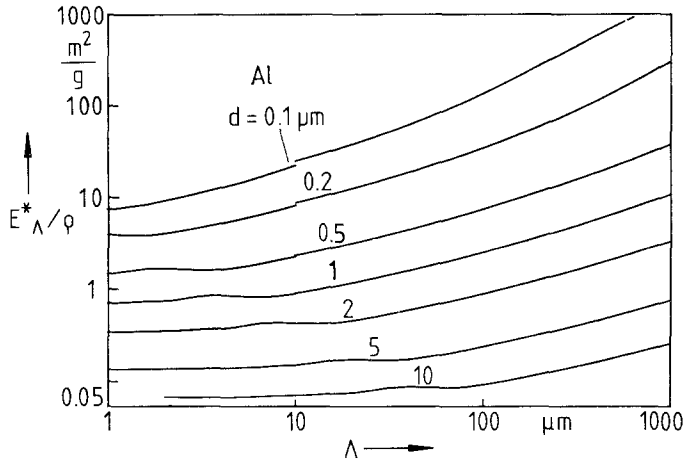

(b)

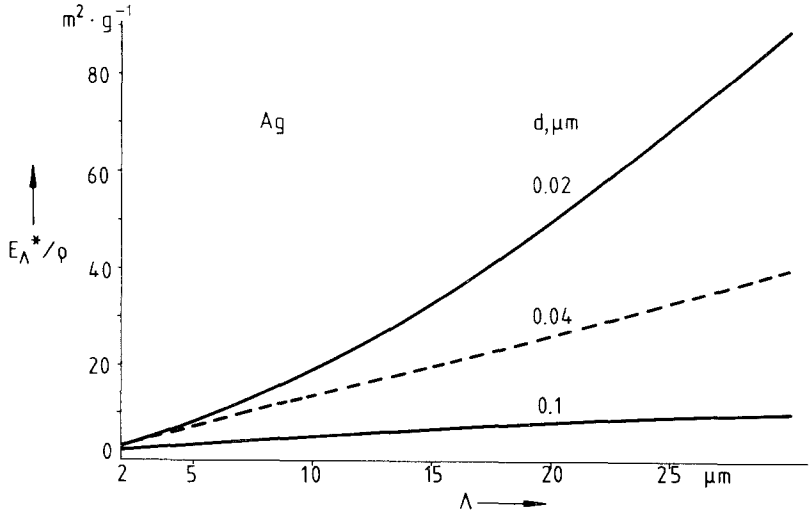

(c)

Figs. 2a, b, c (*continued*)

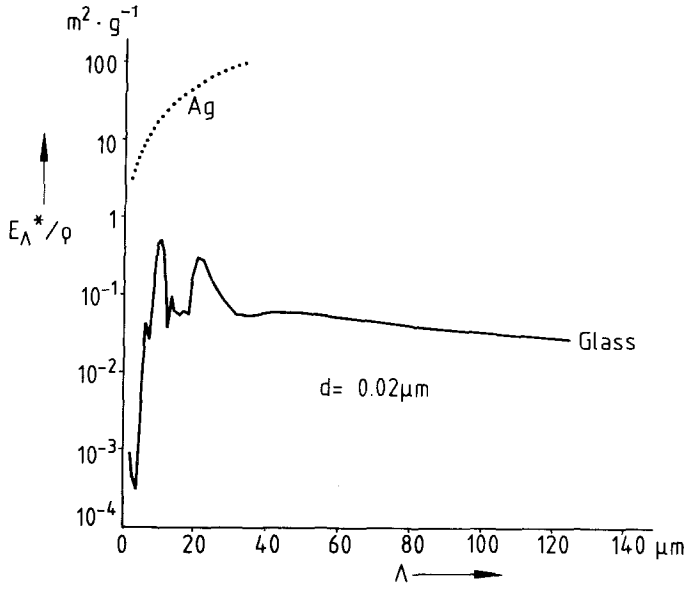

Fig. 3. Effective values E_Λ^*/ρ of the specific extinction coefficient E_Λ/ρ of the fibers made of glass (logarithmic scale) in dependence of wavelength, Λ, and for a fixed fiber diameter, d. ρ denotes the density of the fibers (the E_Λ^*/ρ of Ag are given for comparison).

values for conducting and glass fibers in dependence of wavelength, Λ, and diameter, d. Although the corrections introduced in Eq. (5) are strong, the E_Λ^*/ρ of thin conducting fibers is still at least two orders of magnitude larger than the corresponding value for glass fibers.

In order to use Eq. (4a) for the calculation of λ_{rad}, we need the Rosseland mean $E_R^*(T)$ of the effective extinction coefficient E_Λ^*. If e_b and $e_{\Lambda b}$ denote the total and spectral hemispherical emissive power of a blackbody, E_R^* is defined by

$$\frac{1}{E_R^*(T)} = \frac{\int (1/E_\Lambda^*)(\partial e_{\Lambda b}/\partial e_b)\, \partial \Lambda}{\int (\partial e_{\Lambda b}/\partial e_b)\, \partial \Lambda} \tag{7}$$

Figures 4 and 5 show the calculated $E_R^*(T)/\rho$ for metal and glass fibers in dependence of temperature, T, and diameter, d. The calculated $E_R^*(T)/\rho$ values for glass fibers in Fig. 5 are in very good agreement with experimental values extracted from calorimetric or extinction measurements in Refs. 13 and 14. Assuming a density of, e.g., 250 kg · m^{-3} for metal fibers (Ag) or glass fibers (corresponding to porosities of 0.98 and 0.84, respectively), we have temperature-dependent, wavelength-averaged, effective

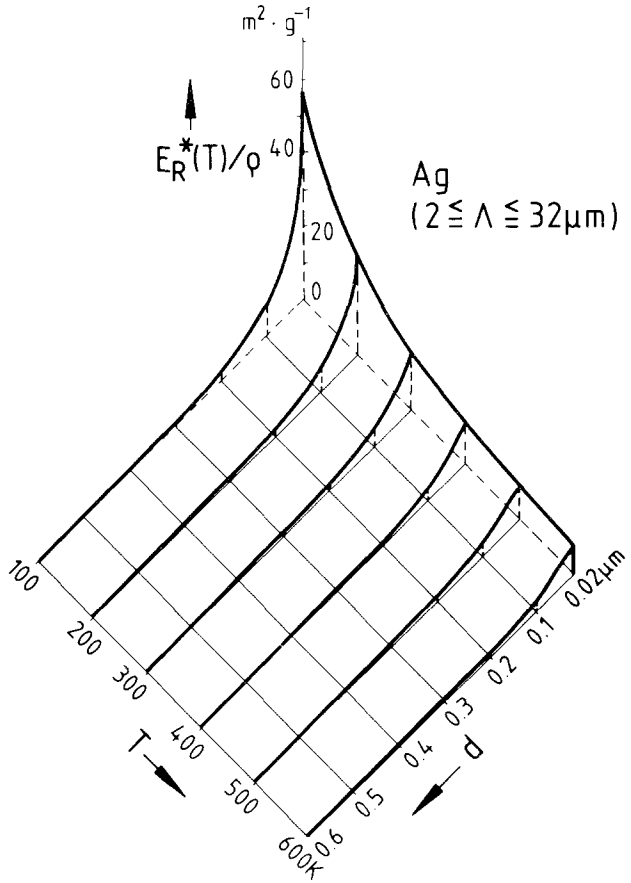

Fig. 4. Effective values $E_R^*(T)/\rho$ of the Rosseland mean of the specific extinction coefficient E_Λ^*/ρ of fibers made of a metal (Ag) in dependence of temperature, T, and fiber diameter, d (the wavelength average has been calculated within $2 \leqslant \Lambda \leqslant 32$ μm).

extinction coefficients $E_R^* = 1.125 \times 10^6\ m^{-1}$ for the metal fiber and $\sim 1.5 \times 10^3\ m^{-1}$ for the glass-fiber insulation at $T = 300$ K and for $d = 0.1$ μm. For $d = 0.5$ μm, the E_R^* value of the metal fiber is still larger than $10^5\ m^{-1}$ so that the above-mentioned limit of $10^5\ m^{-1}$ could be achieved if metal fibers of this diameter were available. Note the huge increase in the E^*/ρ at very small fiber diameters and at low temperatures in Fig. 4. Similar results are to be expected for highly reflective Al fibers [note that the ρ_0 of Al is considerably smaller than that of Ag in Eq. (3), whereas the Q_{ext} should be comparable] if the Al surface is clean.

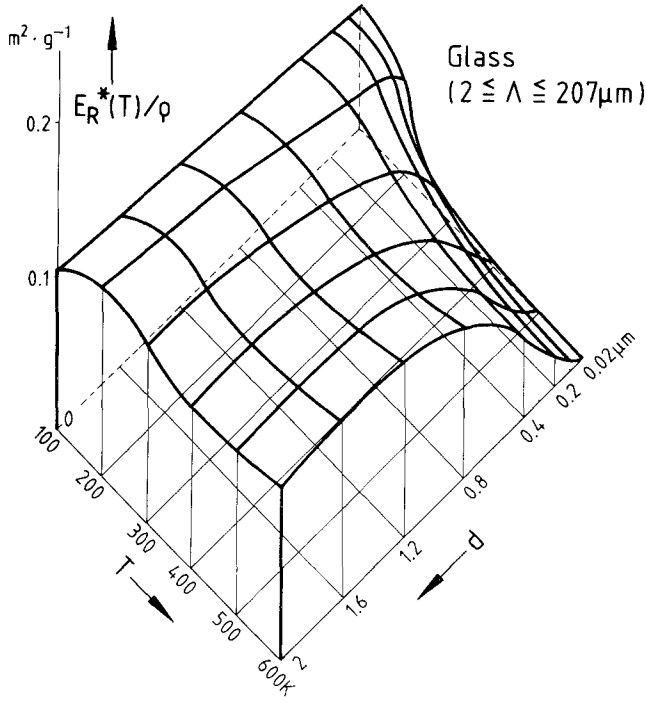

Fig. 5. Effective values $E_R^*(T)/\rho$ of the Rosseland mean of specific extinction coefficient E_Λ^*/ρ for glass fibers in dependence of temperature, T, and fiber diameter, d (wavelength average between $2 \leqslant \Lambda \leqslant 207\ \mu m$).

A general theory for dependent scattering in fiber-like media does not exist. Common to most recent work on the problem which parameters influence the onset of dependent scattering in media of spherical particles is the ratio of particle clearance c to wavelength Λ. Hottel et al. [16] report for the effective scattering cross section Q_{ext}^{eff} of *spherical* particles the relation

$$\log \log(Q_{ext}/Q_{ext}^{eff}) = 0.25 - 5.1\ c/\Lambda \tag{8}$$

It is not at all clear that this relation is also applicable in the case of cylindrical particles. For the clearance c, only tentatively can we use an expression developed [17] for the effective diameters of void spaces in *fiber* insulations from statistical assumptions on collisions between gas molecules and fibers, $c = 0.785\ d/(1-\Pi)$. Using this relation in Eq. (8) and $d \geqslant 0.8\ \mu m$ and $\rho/\rho_0 \leqslant 0.05$ there is little reduction of Q_{ext}^{eff}/Q_{ext}. If $d \leqslant 0.1\ \mu m$, however, the corrections could be very large if $\rho/\rho_0 \geqslant 0.01$.

Apparently, the full potential for radiation extinction by totally reflecting thin fibers is exploited only if the fibers are strongly dispersed. On the other hand, an experimental study of the onset of dependent scattering in fibrous media (performed only very recently [15]) shows that the extinction coefficient is reduced by a factor of two only when the glass fiber density is increased above $1600\,\mathrm{kg/m^3}$. However, the cross sections of totally reflecting cylindrical particles are, by orders of magnitude, larger than those of pure glass fibers, so that shading of the cross sections could occur at considerably lower densities. Further investigations are necessary to clarify this situation.

3. PREPARATION OF METAL COATINGS

Since pure metal fibers with diameters, d, below $0.5\,\mu\mathrm{m}$ were not available, we investigated different deposition techniques to prepare metal-coated dielectric fibers for a simulation of the radiative properties of very thin, infinitely long, metal cylinders. A candidate for Al deposition on thin fibers is, besides the usual evaporation processes, low-pressure CVD.

The Al deposition on fiber substrates [18] was carried out by thermal decomposition of triisobutylaluminum (TIBA). TIBA is a pyrophoric clear liquid which decomposes at temperatures above 250°C in two steps according to the reactions

$$[(CH_3)_2\,CH\text{–}CH_2]_3\,Al \xrightarrow{100\ 150^\circ C} [(CH_3)_2\,CH\text{–}CH_2]_2\,AlH + (CH_3)_2\,C=CH_2$$

and

$$[(CH_3)_2\,CH\text{–}CH_2]_2\,AlH \xrightarrow{250^\circ C} Al + 3/2H_2 + 2(CH_3)_2=CH_2$$

A low-pressure CVD apparatus was constructed with stainless-steel components because of the dangerous properties of the starting compound TIBA. The leakage rate of the deposition apparatus was in the range of $10^{-3}\,\mathrm{Pa\cdot s^{-1}}$. For kinetic control measurements, deposition experiments were carried out on carbon fibers. An activation energy of $E_A = 65\,\mathrm{kJ\cdot mol^{-1}}$ for Al deposition was found in the reaction-controlled range of $250^\circ C \leqslant T \leqslant 350^\circ C$ and at a total pressure of 50 Pa.

Deposition rates of $1.5\,\mu\mathrm{m\cdot h^{-1}}$ with a good throwing power were obtained in the reaction-controlled region. At temperatures higher than 350°C the deposition is controlled by diffusion of the gas into the fiber

bundle, and therefore less aluminum could be deposited in the middle of the bundle in comparison to other filaments.

Although Ref. 19 reports that thin dielectric fibers with diameters $d \leqslant 0.1$ μm can be prepared, fibers of that small diameter were not available up to now. Therefore as a first attempt, a glass-fiber insulation with a mean fiber diameter $d = 3$–4 μm was CVD coated with Al in order two investigate whether CVD is a suitable deposition process for felts or blankets of fibers.

Figure 6a (scanning micrograph of coated fibers) shows that the fibers are completely covered by small Al crystals. The resulting rough fibers surfaces little resemble the idealized assumption made for the calculations in section II. On the other hand, the electrical conductivity of such CVD coatings is high as is well known from experiments with Al-coated carbon fibers prepared for superconducting wires. Nevertheless, a considerable improvement was achieved when the above-given CVD process was modified by the inclusion of a nucleation promoting step (exposure to $TiCl_4$ vapor; see Fig. 6b).

Although the blankets had a thickness of about 15 mm, the glass fibers

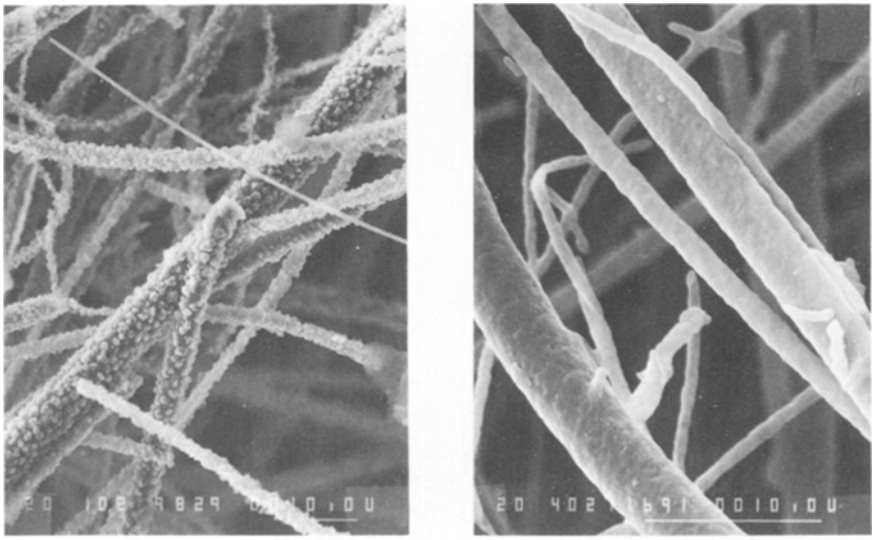

(a) (b)

Fig. 6. Scanning micrograph of glass fibers coated with Al in a CVD process using TIBA (a) and additional exposure to $TiCl_4$ vapors (b; this sample was prepared by Mr. B. G. Sluijk, ASM, Bilthoven, NL) (the length of the horizontal bars indicates 10 μm).

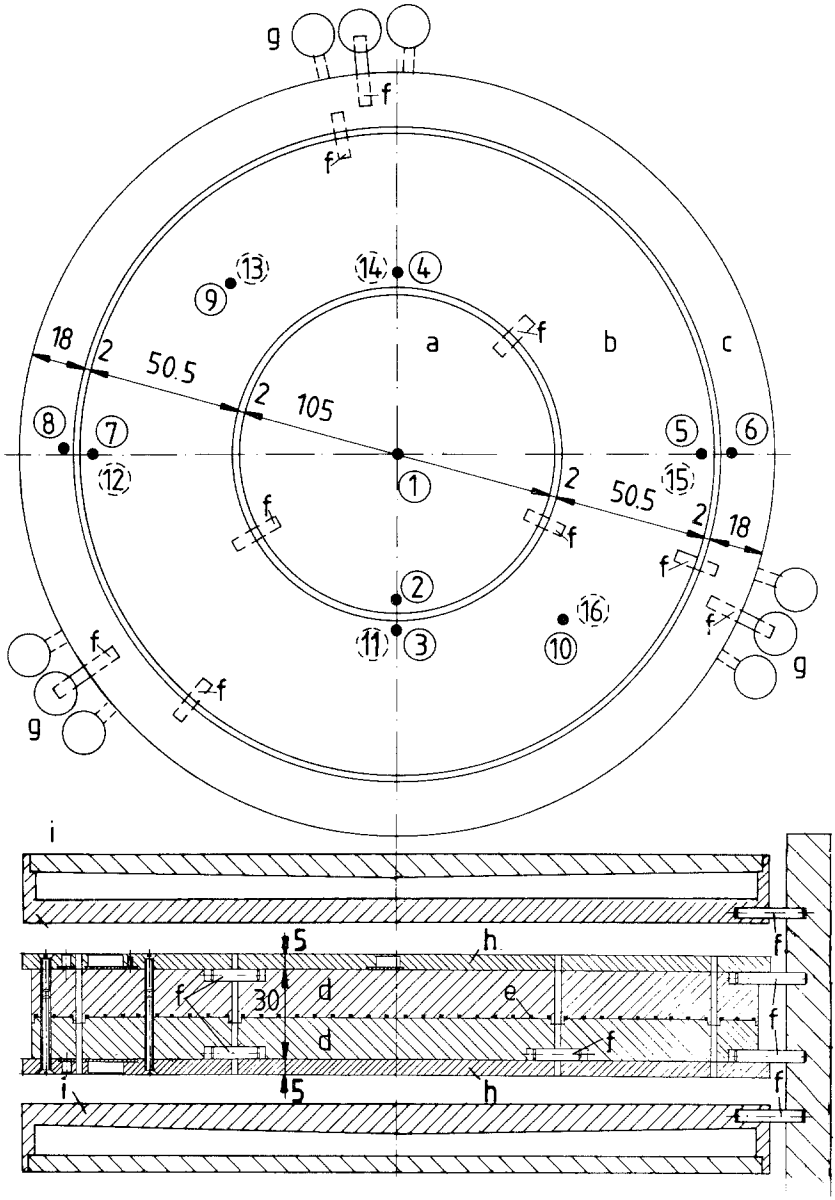

Fig. 7. Top view (above) and cross section (below) of the guarded hot-plate apparatus used for the measurement of the total thermal conductivity. (a) Metering section; (b, c) inner and outer guard ring; (d) half-plates (sandwich); (e) heating coil; (f) ceramic supports; (g) pillars for mounting (separately) hot and cold plates; (h) plates carrying temperature sensors (platinum resistance thermometers with four-conductor cables); (i) cooling plates. Filled circles and numbers (within circles) denote positions of temperature sensors (numbers in dashed circles refer to a position at the lower side of the hot plate system). Measures are in millimeters. All plate elements are made from Cu. Standard deviations of temperature distributions in the metering section and inner guard ring were about 0.2 K; differences between mean values of temperatures of the order of 1/100 K in the stationary state.

were successfully coated regardless of the depths of the layers. This is a considerable improvement compared to physical deposition techniques. The thickness of the coatings is at least 0.5–1 μm.

4. EXTINCTION AND THERMAL CONDUCTIVITY MEASUREMENTS

Spectral extinction measurements were performed with the device described in Ref. 13. For stationary calorimetric measurements at low temperature, a guarded hot-plate device with a metering section of 105-mm diameter and two guard rings of 51 and 18 mm was used (Fig. 7). Its plate geometry has been optimized following the recommendations made in Ref. 20. Cooling of the reference plates was made with LN_2 under static pressure. The whole experiment (reading of resistances and conversion to temperatures, running three calibrated DC power supplies, storage and plotting of the data) was completely computerized using a 16 bit on-line computer, a microprocessor multimeter, and scanners.

Figure 8 shows spectral values of E_Λ/ρ measured with completely or partly metallized glass fibers. It is obvious that the goal 0.5 $m^2 \cdot g^{-1}$ (with $\rho = 200\ kg \cdot m^{-3}$) cannot be reached with the large fiber diameter. Since the transmission window in pure glass fibers between 6 and 8 μm has been

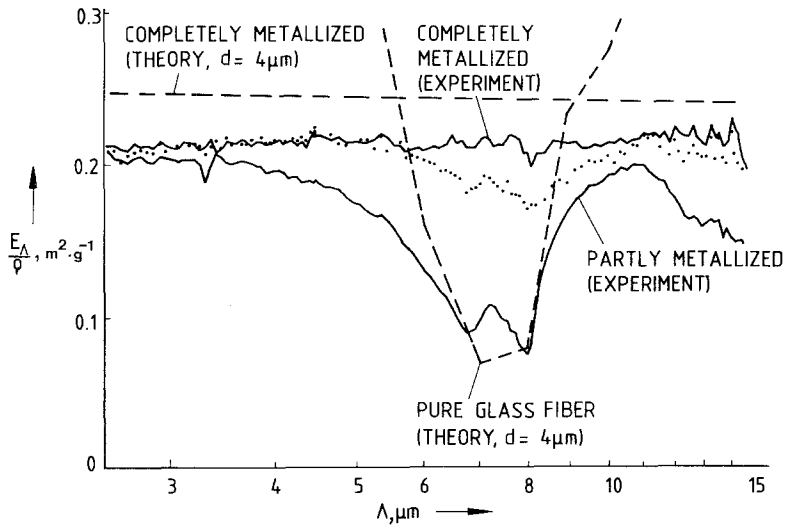

Fig. 8. Measured spectral extinction coefficients E_Λ/ρ of completely and partly Al-coated glass fibers (from Fig. 6a) (the filled circles denote a sample taken from the center of the glass-fiber felt) and theoretical curves.

closed completely by the Al coating and because of a reduction of forward scattering obtainable with metal fibers (see Refs. 12, 15), the Rosseland mean E_R^*/ρ (Fig. 9) has been increased by a factor of 1.5 to 2 in the temperature range $100 \leqslant T \leqslant 900$ K. The observed nearly constant spectrum E_Λ/ρ for metal-coated fibers is confirmed by a calculation for $d = 4$-μm fiber diameter. Although the fiber surfaces are rough (Fig. 6a), it seems that a crystal structure of the upper layers does not seriously influence the idealized assumptions made for the Mie calculations. Another calculation of the E_Λ/ρ of *spherical* metal particles does *not* reproduce the nearly constant experimental spectrum in that range of wavelengths.

Comparison of the experimental extinction spectrum of completely metallized fibers (Fig. 8) with the extinction spectra of glass fibers highly doped with Fe_3O_4 or soot (Figs. 10a and b, which still exhibit the well-known transimission window) demonstrates that the metal coating covers the dielectric core totally.

Experimental values of the total thermal conductivity, λ, versus T^{*3}, are shown in Fig. 11 for metal-coated and pure glass fibers in vacuum. Apparantly, the metal coating does not seriously increase the low λ_s value

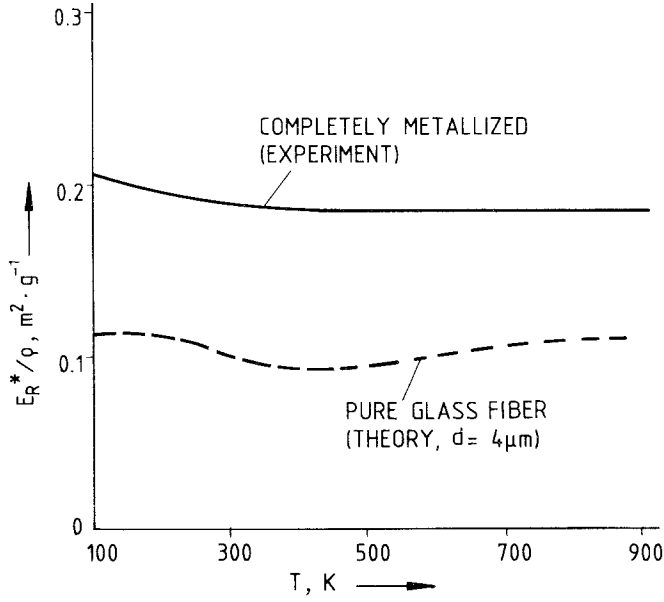

Fig. 9. Rosseland mean E_R^*/ρ of spectral extinction coefficients E_Λ/ρ from Fig. 8.

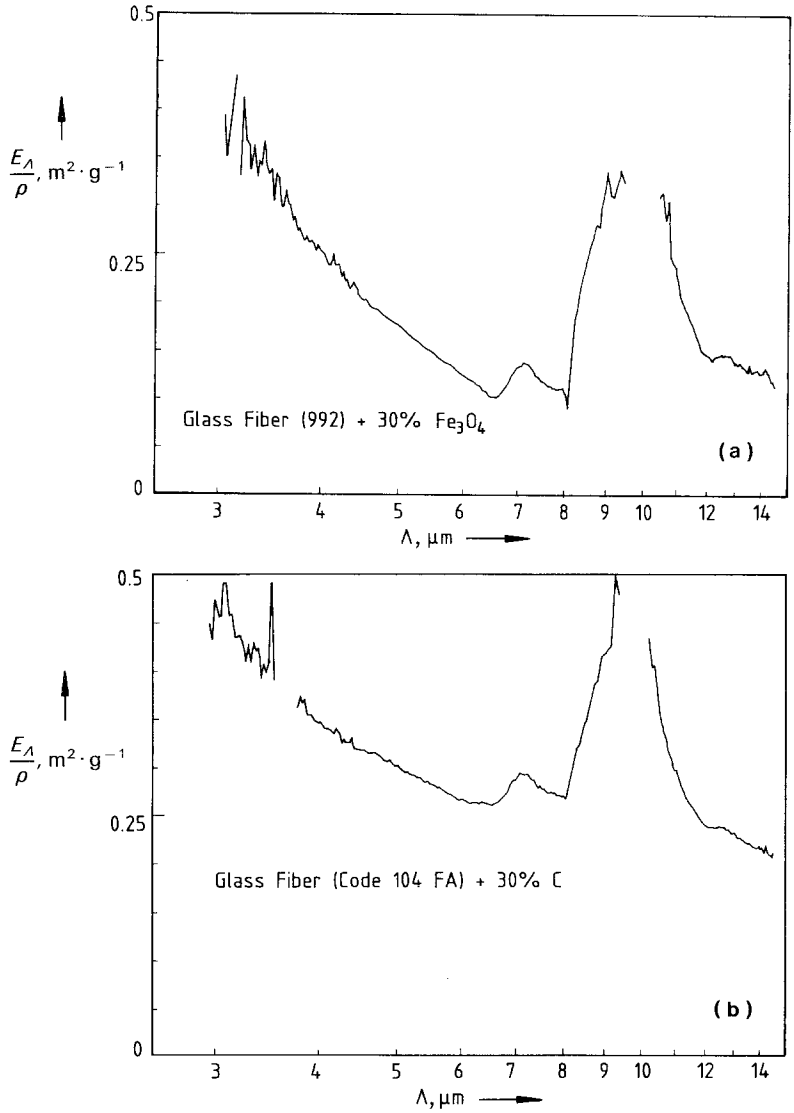

Fig. 10. Experimental values of E_Λ/ρ of glass fibers doped with (a) Fe_3O_4 and (b) soot (30 wt%); fiber diameters are between 3 and 5 μm.

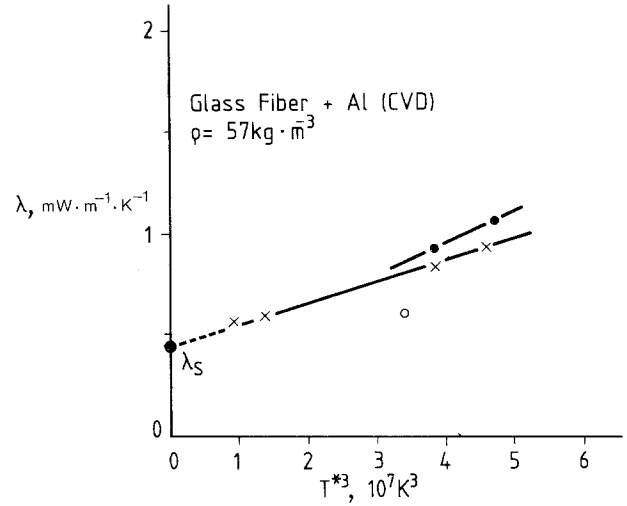

Fig. 11. Total thermal conductivity, λ, versus radiation temperature T^{*3} of metal-coated (Al) glass fibers (crosses) and pure glass fibers (circles) in vacuum (residual gas pressures: crosses and open circle, 0.1 Pa; filled circles, 0.8 Pa). The filled circle at the intercept is obtained from an extrapolation of the least-squares fit to the experimental values (solid line) to $\lambda_S = \lambda(T^{*3} = 0)$.

of pure glass fibers. This finding strongly increases the potential for a reduction of the total λ exclusively by minimizing the radiative heat flow $\dot{q}_{\text{rad}}$.

Our next step will be preparation of metallized glass or ceramic fibers with diameters below 1 μm by modified CVD processes.

REFERENCES

1. E. M. Sparrow and N. Cur, *J. Heat Transfer* May: 232 (1976).
2. G. R. Cunnington and C. L. Tien, *Adv. Cryog. Eng.* **18**:103 (1972); C. K. Chan and C. L. Tien, Combined Radiation and Conduction in Packed Spheres, Proc. 5th Int. Heat Transfer Conf., Vol. 1, R2.2, p. 72 (1974).
3. M. G. Kaganer, *Thermal Insulation in Cryogenic Engineering* (Israel Prog. Sci. Transl., Jerusalem, 1969), pp. 21–24.
4. M. Kerker, *The Scattering of Light* (Academic Press, New York, 1969), pp. 286–289.
5. K. Y. Wang and C. L. Tien, *J. Quant. Spectrosc. Radiat. Transfer* **30**:213 (1983).
6. C. F. Bohren and D. R. Huffmann, *Absorption and Scattering of Light by Small Particles* (John Wiley & Sons, New York, 1983).
7. R. Caps, J. Fricke, and H. Reiss, *High Temp. High Press.* **17**:303 (1985).
8. M. Kerker, ibid., pp. 261–262.

9. H. Reiss, Radiative Transfer in Disperse Non-Transparent Media, Thesis for Habilitation (1985), Univ. of Würzburg, FRG, to be published.
10. M. A. Ordal, L. L. Long, R. J. Bell, S. E. Bell, R. R. Bell, R. W. Alexander, Jr., and C. A. Ward, *Appl. Opt.* **22**:1099 (1983).
11. C. K. Hsieh and K. C. Su, *Solar Energy* **22**:37 (1979).
12. H. Reiss and B. Ziegenbein, *Int. J. Heat Mass Transfer* **28**:1408 (1985).
13. R. Caps, A. Trunzer, D. Büttner, J. Fricke, and H. Reiss, *Int. J. Heat Mass Transfer* **27**:1865 (1984).
14. H. Reiss and B. Ziegenbein, *High Temp. High Press.* **17**:403 (1985).
15. R. Caps, *Strahlungswärmeströme in evakuierten thermischen Superisolationen*, Doctor Thesis, Univ. of Würzburg, FRG (1985), Rep. No. E 12-1285-1 (1985).
16. H. C. Hottel, A. F. Sarofim, W. H. Dalzell, and I. A. Vasalos, *AIAA J.* **9**:1895 (1971).
17. J. D. Verschoor and P. Greebler, *J. Heat Transfer (Transact. ASME)* **74**:961 (1952).
18. F. Schmaderer, G. Wahl, M. Dietrich, and C.-H. Dustmann, Preparation of Al-Stabilized Superconducting $NbC_{1-y}N_y$-Carbon Fibers, Proc. 9th Int. Conf. Chem. Vapor Deposit., Cincinnati (1984) (Electrochemical Society, Pennington, N.J., 1984), pp. 663–672.
19. N. B. Scheffel, *TAPPI* **58**:56 (1975).
20. K. H. Bode, *Int. J. Heat Mass Transfer* **23**:961 (1980).